

# Finite Element Modeling for Prediction of Cutting Forces during Micro Turning of Titanium Alloy

Jagadesh T<sup>1</sup>, Samuel G L<sup>2\*</sup>

<sup>1</sup>Department of Mechanical Engineering, Indian Institute of Technology Madras, Chennai, India, 600036,

<sup>1</sup>E-Mail: jagadeshvel@gmail.com, <sup>2</sup>Email: samuelgl@iitm.ac.in

## Abstract

Micromachining of industrial products, is playing an important role in manufacturing of axi-symmetric miniaturized parts especially in biomedical and aerospace applications. This paper presents the development of 3D oblique finite element modeling for prediction of cutting forces, thrust force, feed force, and tool chip interface temperature during micro turning process. Titanium alloy (Ti6Al4V) and Coated carbide tool (TiN/AlTiN) is considered as work and tool material respectively. Johnson-Cook material model with strain gradient plasticity is used to represent the flow stress of the work material. When uncut chip thickness is equal to or less than the edge radius, thrust force is dominant over the cutting force due to rubbing and ploughing action. When cutting speed increases there is decrease in cutting force due to thermal softening effect. When depth of cut and uncut chip thickness is less than edge radius there is increase in specific cutting energy due to material strengthening effects. Tool chip interface temperature increases by increasing the cutting speed. Simulated cutting force values agree well with the experiment values.

*Key words:* FEM, Cutting forces, edge radius.

## 1. Introduction

Titanium alloys have been widely used in biomedical products due to superior properties such as biocompatibility, high strength to weight ratio, and corrosion resistance. Machining of titanium alloy is difficult due to low thermal conductivity, low elastic modulus and high chemical reactivity with tool material Yang and Liu (1999). Several researches have tried with different coated tools to minimize the tool wear and for improving the accuracy of the component Ozelet *et al.* (2010), Jaffery and Mativenga (2012). In the present paper, coated carbide insert (TiN/AlTiN) is being used as a tool to machine titanium alloy (Ti6Al4V). The advantage of such coating is to reduce the friction and adhesion between chip and cutting tool. In addition to that AlTiN has good oxidation resistance, wear resistance and high chemical stability at high temperatures due to the formation of Al<sub>2</sub>O<sub>3</sub> film.

The mechanism of material removal in micromachining is different from macro machining due to size effect. Finite element model is used to predict the cutting forces, tool wear in advance to eliminate problem during actual machining process that leads to reduce the experimentation cost. Woonet *et al.* (2008) developed finite element model to predict the influence of tool edge radius on tool chip contact length and contact force. Ozelet *et al.* (2011) investigated FEM for prediction of forces, temperature and wear rate during micro milling of titanium alloy with carbide and

cBN coated tool. Rao and shunmugam (2012) developed analytical model for the prediction of forces in micro end milling process with consideration of edge radius and material strengthening effects. Liu and melkote (2004) investigated material strengthening mechanisms and suggested that decrease in secondary deformation zone temperature, and strain gradient are the reason for material strengthening.

Several researches investigated on Finite element model (FEM) for macromachining of titanium alloy. Umbrello (2008) studied finite element simulation of titanium alloy (Ti6Al4V) using three different Johnson Cook constitutive model parameters. Results suggested that Lee and Lin (1998) parameters shows good agreement of cutting force and chip morphology with experiments during conventional and high speed machining. Sima and Ozel (2010) investigated strain softening, temperature dependent flow softening, and flow softening at high strain values in modified Johnson Cook constitutive model. Results suggested that flow softening at high strain values predicted accurately with experiment values. Karpal (2011) analyzed temperature dependent flow softening of Ti6Al4V using 2D FEM. Results suggested that flow softening occurs at 350 °C that is below the recrystallization temperature. Ti6Al4V with different initial microstructures are needed to address this problem. Shao *et al.* (2010) developed finite element model for prediction of cutting temperature and tool wear depth considering thermodynamically constitutive equation. Ozel (2009) investigated

influence of micro edge geometry (chamfer insert, uniform hone insert, variable hone insert, waterfall hone insert) on forces, stress, friction and tool wear in PcBN tool. Results suggested that variable micro geometry insert has reduced tool wear, heat generation and less plastic strain.

Most of the work done in the literature study is 2D and 3D orthogonal FEM for macro machining. To get the actual cutting process, 3D oblique finite element model has been developed in the present investigation. There are very few investigations made so far on simulation of micro turning of Titanium alloy. This paper is essential to understand the mechanism of material removal at the micro scale.

## 2. Methodology

### 2.1 Finite element model

There are three formulations used in the finite element model of machining process: Lagrangian, Eulerian, or Arbitrary Lagrangian Eulerian. Material being removed from the workpiece is exposed to severe plastic deformation and it causes distortion of elements during FEM simulation. Therefore mesh regeneration in the workpiece is needed. In addition this chip separation criteria must be provided in Eulerian approach. To overcome this problem, in this paper finite element simulation has been carried out by implicit Lagrangian method in which the chip is formed by continuous remeshing using DEFORM 3D software. Ozelet *al.* (2011) studied the FEM of machining of inconel 718 by using two different FE software. Results suggested that predicted cutting forces, cutting temperature, strain, and stress values are almost similar in both DEFORM 3D and ABAQUS/Explicit.

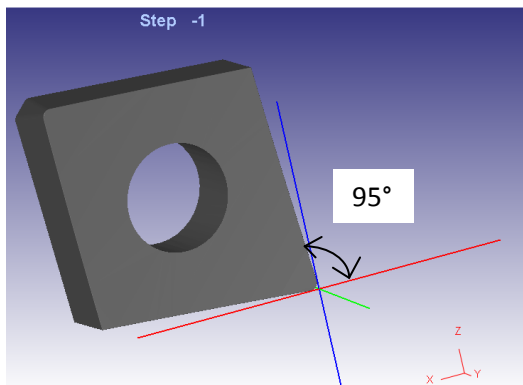


Figure 1 Oblique cutting

Figure 1 shows the oblique cutting where cutting edge is inclined at 95° to the feed velocity. Tool is considered

as rigid and workpiece is considered as viscoplastic material. To get the influence of edge radius a fine mesh density is given at the tip of the tool is shown in figure 2. The edge radius of the cutting insert is 15 μm is shown in figure 6.

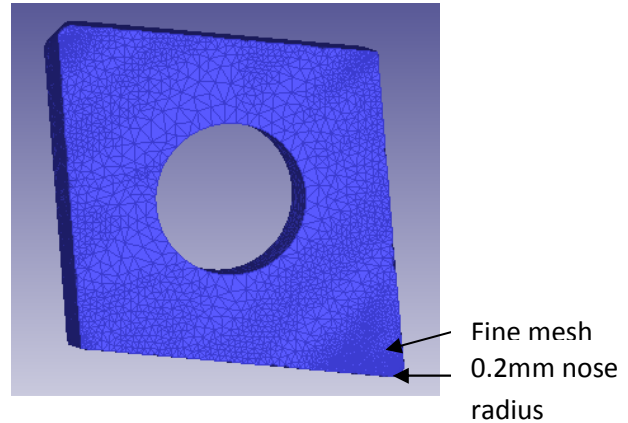


Figure 2 Geometry of insert with finite element mesh

Minimum element size of the workpiece is 0.002mm given in all simulation conditions. The shape of the element is four node tetrahedron element. Figure 3 shows the simplified model of workpiece fixed at bottom portion in X,Y, and Z directions. In the present study uncut chip thickness is assumed to be 10, 15, 20 microns. Figure 4 shows coating of AlTiN and TiN over carbide tool.

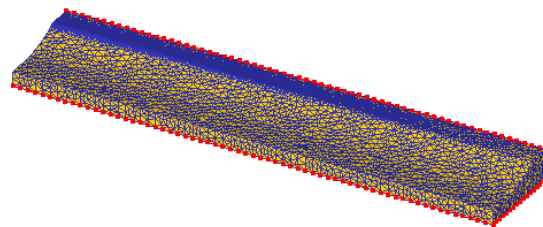


Figure 3 Workpiece fixed at bottom portion

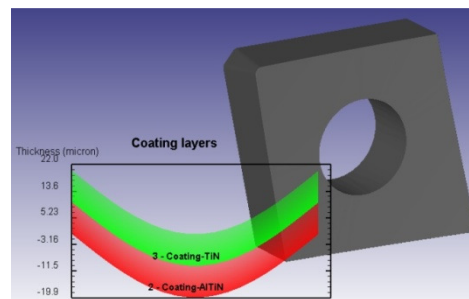
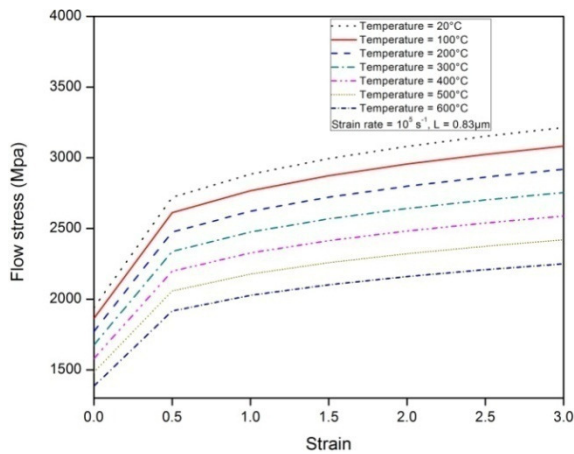


Figure 4 Coated carbide insert

## 2.2 Material modeling

$$\sigma = (A + B\epsilon^n) \left( 1 + C \ln \frac{\dot{\epsilon}}{\dot{\epsilon}_0} \right) \left( 1 - \left( \frac{T - T_o}{T_m - T_o} \right)^m \right) \left( 1 + \frac{18a^2 b G^2}{L \left( (A + B\epsilon^n) \left( 1 + C \ln \frac{\dot{\epsilon}}{\dot{\epsilon}_0} \right) \left( 1 - \left( \frac{T - T_o}{T_m - T_o} \right)^m \right) \right)^2} \right)^{1/2} \quad (1)$$

where (A) yield strength of the material, (B) strain hardening modulus, (C) strain rate sensitivity coefficient, ( $\epsilon$ ) plastic strain, ( $\dot{\epsilon}$ ) strain rate, ( $\dot{\epsilon}_0$ ) reference plastic strain rate, (T) Workpiece temperature, ( $T_m$ ) Melting temperature, ( $T_o$ ) Room temperature, (m) thermal softening coefficient, (n) Hardening coefficient, (G) shear modulus, (L) characteristic length in strain gradient plasticity model, (b) magnitude of burger vector, (a) constant. The optimized material constant for John and cook model are;  $A = 782.7\text{MPa}$ ,  $B = 498.\text{MPa}$ ,  $C = 0.028$ ,  $m = 1$ ,  $n = 0.28$ ,  $T_o = 20^\circ\text{C}$ ,  $T_m = 1660^\circ\text{C}$ . Modified Johnson–Cook material model with strain gradient plasticity is used to represent the flow stress of the work material as shown in Equation 1 Shen and Ding (2013).



**Figure 5 Variation of flow stress with strain at various temperatures**

Figure 5 shows the variation of flow stress with strain at various temperatures. Figure 6 shows the 3D oblique model of tool and workpiece along with the chip formed during oblique finite element cutting model. The reason for the saw tooth chip formation in machining of titanium alloy is due to adiabatic shear sensitivity Wan *et al.*(2012).

## 2.3 Friction modeling

Shear friction law and coloumb friction law are used to represent the friction between tool and chip interface.

$$m = \frac{\tau}{k} \quad (2)$$

where,  $m$  = shear friction factor.

$\tau$  = frictional shear stress.

$k$  = work material flow stress.

A constant shear friction factor  $m = 0.95$  is used in all simulation conditions Ozelet *al.* (2010).Table 1 shows the thermo mechanical properties of tool and workpiece material. The formula for calculating shear frictor is shown in Equation 2, and specific cutting energy is shown in Equation 3.

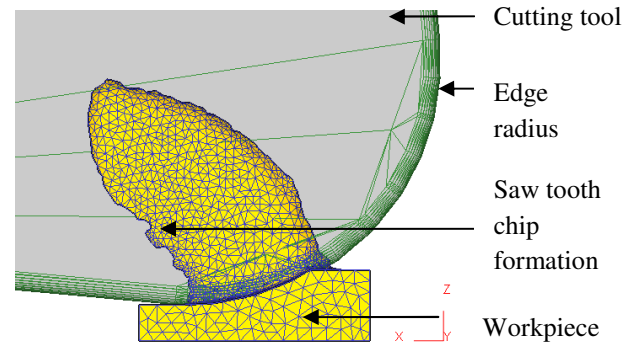


**Figure 6 Finite element model**

$$\text{Specific cutting energy} = \frac{F_c \times V_c}{\text{DOC} \times V_c \times f} \quad (3)$$

$F_c$  = Cutting force, N

$V_c$  = Cutting speed, m/min

DOC= Depth of cut,  $\mu\text{m}$

$f$  = feed,  $\mu\text{m}/\text{rev}$

**Table 1. Mechanical and thermal properties of tool and work material.**

Property	Ti6Al4V	WC-Co	AlTiN	TiN
Youngs modulus, Mpa	$(0.7412 * T) + 113375$	$5.e^5$	$560e^3$	$251e^3$
Thermal conductivity $\text{Wm}^{-1}\text{C}^{-1}$	$7.039e^{0.0011 * T}$	$0.042 * T + 36$	$0.008 * T + 11.95$	$0.008 * T + 19.8$
Thermal expansion $\text{mm mm}^{-1}\text{C}^{-1}$	$3.10^{-9} * T + 7.10^{-6}$	$4.7e^{-6}$	$9.4e^{-6}$	$9.4e^{-6}$

Heat capacity Nmm <sup>-2</sup> C <sup>-1</sup>	2.24e <sup>0.0007*T</sup>	0.000 5*T +2.07	0.000 3*T +0.57	3
Poisson's ratio	0.342	0.25	0.25	0.25

Yen *et al.*(2004), Ozelet *al.*(2010),Jaffery and Mativenga (2012).

### 3. Results and discussion

#### 3.1 Effect of forces on edge radius

It is observed from the simulation results that, when the cutting edge radius is equal to or less than the

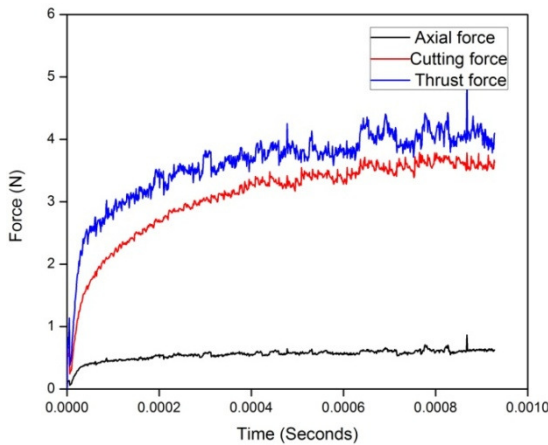


Figure 7 Variation of forces with time at 19m/min, 10µm/rev, 10µm depth of cut.

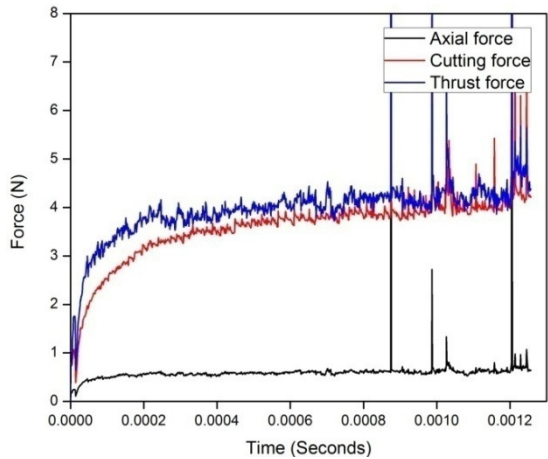


Figure 8 Variation of forces with time at 19m/min, 15µm/rev, 10µm depth of cut.

uncut chip thickness thrust force is more than the cutting force due to rubbing and ploughing action is shown in the figure 7 and 8. When uncut chip thickness is greater

than edge radius, cutting force is dominant over thrust force due to shearing action is shown in the figure. 9.

#### 3.2 Effect of cutting forces on cutting speed

When cutting speed increases, from 19m/min to 37m/min there is sudden decrease in cutting force due to increase of temperature in the cutting zone. with further increase of cutting speed there is gradual decrease of cutting force due to thermal softening effect. When cutting speed increases from 57m/min to 75m/min the value of cutting force and

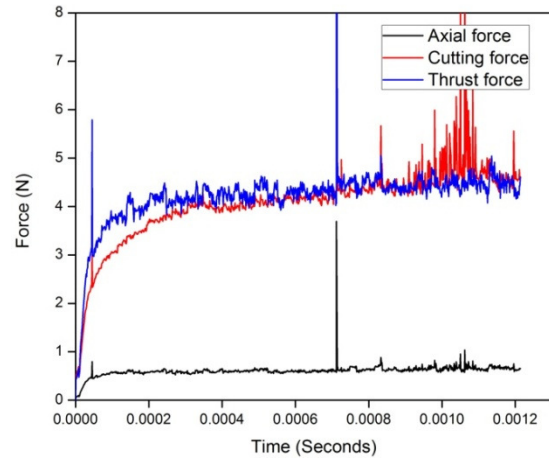


Figure 9 Variation of forces with time at 19m/min, 20µm/rev, 10µm depth of cut.

thrust force coming close, and indicates that it is not favorable condition for machining. There is no much variation in axial force when cutting speed increases from 19m/min to 75m/min. Figure 10 shows the variation of forces with time at 57m/min, 20 µm/rev, and 30µm depth of cut.

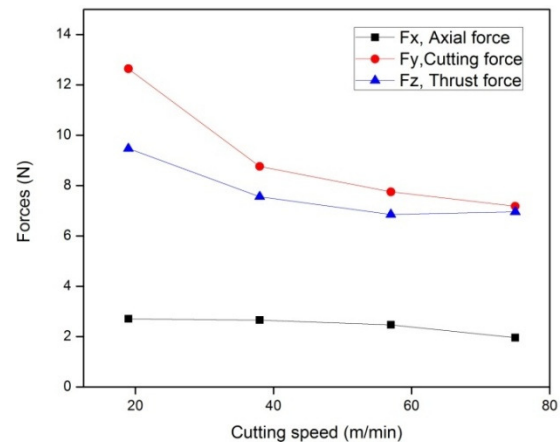


Figure 10 Variation of forces with time at 57m/min, 20µm/rev, 30µm depth of cut.

### 3.3 Effect of cutting forces on feed rate and depth of cut.

Figure 11 shows the variation of cutting force with feed rate at 19m/min. Cutting force increases with increase of feed rate and depth of cut due to increased volume of material removal.

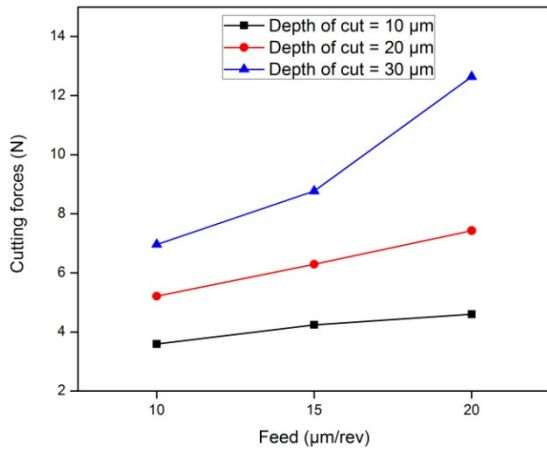


Figure 11 Variation of cutting force with feed rate at 19m/min.

### 3.4 Specific cutting energy

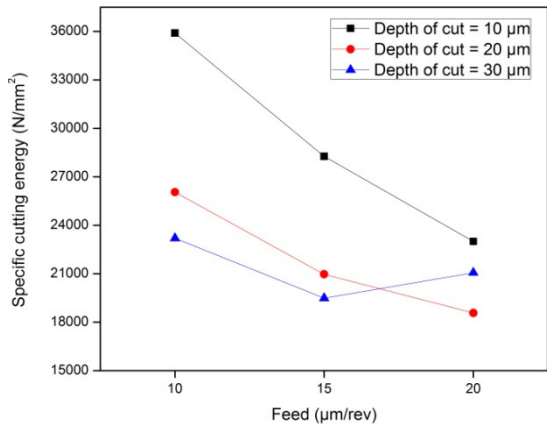


Figure 12 Variation of specific cutting energy at 19m/min.

Figure 12 shows the variation of specific cutting energy at various feed rates. When uncut chip thickness is less than the edge radius there is increase in specific cutting energy due to strain gradient induced material strengthening effects Liu and melkote (2004). Figure 13 shows the variation of tool chip interface temperature with cutting speed. Since titanium alloy have low thermal conductivity, heat generated during machining are not dissipated,

and hence there is increase of tool chip temperature by increasing the cutting speed.

### 3.5 Finite element model validation

Micro turning of Ti6Al4V have been carried out using coated carbide tool (AlTiN/TiN) in micro turning setup at IIT Madras. Experiments were conducted by varying cutting speed, feed and depth of cut. Simulated force values are compared with experimental values.

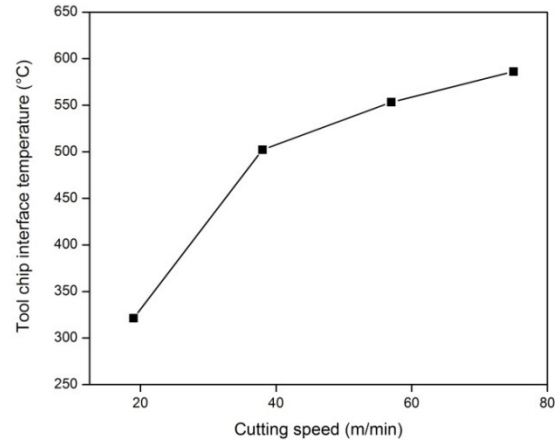


Figure 13 Variation of tool chip temperature with cutting speed at 20 μm/rev, 30 μm depth of cut.

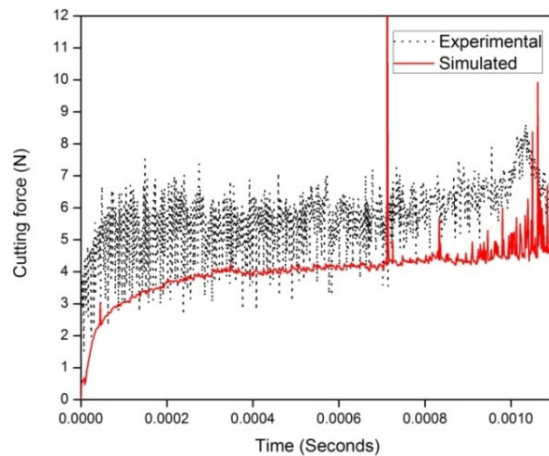
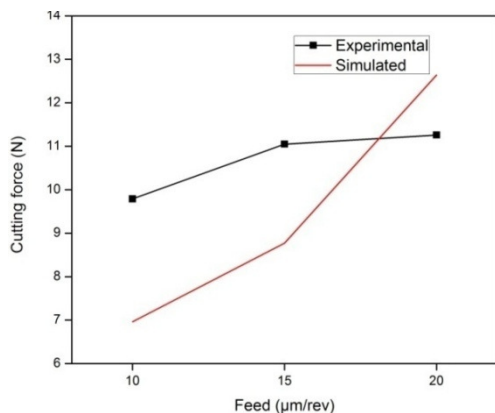


Figure 14 Comparison of experimental and simulated cutting force at 19m/min, 20 μm/rev, 10 μm depth of cut.

Figure 14 shows comparison of experimental and simulated cutting forces with time. Figure 15 shows the comparison of experimental and simulated cutting forces at 19m/min and 30 μm depth of cut.





**Fig.15 Variation of cutting force with feed at 19m/min, 30µm depth of cut.**

#### 4. Conclusion

In this study, 3D oblique process and material strengthening effects have been considered to get the accurate prediction of the cutting forces during micro turning of titanium alloy. Cutting edge radius plays a vital role in the magnitude of cutting forces and mode of material removal. Interface heat generation is predominant at high speed, which leads to thermal softening. At low depth of cut, and uncut chip thickness there is increase in specific cutting energy due to material strengthening effect caused by strain gradient.

#### 5. References

Jaffery, S.I. and Mativenga,P. (2012), Wear Mechanisms Analysis for Turning Ti-6Al-4V Towards the Development of Suitable Tool Coatings,*The International Journal of Advanced Manufacturing Technology*,Vol.58, pp.479-493.

Karpat, Y. (2011), Temperature Dependent Flow Softening of Titanium Alloy Ti6Al4V: An Investigation Using Finite Element Simulation of Machining, *Journal of Materials Processing Technology*,Vol. 211, pp.737-749.

Lee, W.S. and Lin, C.F. (1998), Plastic Deformation and Fracture Behaviour of Ti-6Al-4V Alloy Loaded with High Strain Rate under Various Temperatures,*Materials Science and Engineering: A*,Vol. 241, pp. 48-59.

Liu, K. and Melkote, S.N. (2005), Material Strengthening Mechanisms and Their Contribution to Size Effect in Micro-Cutting, *Journal of Manufacturing Science and Engineering*,Vol.128, pp.730-738.

Ozel, T. (2009), Computational Modelling of 3d Turning: Influence of Edge Micro-Geometry on Forces, Stresses, Friction and Tool Wear in PcBN Tooling,*Journal of Materials Processing Technology*,Vol.209, pp.5167-5177.

Ozel, T.,Sima,M.Srivastava, A.K. and KaftanogluB. (2010), Investigations on the Effects of Multi-Layered Coated Inserts in Machining Ti-6Al-4V Alloy with Experiments and Finite Element Simulations,*CIRP Annals - Manufacturing Technology*,Vol. 59, pp.77-82.

Ozel, T.,Thepsonthi,T.Ulutan,D.andKaftanogluB. (2011), Experiments and Finite Element Simulations on Micro-Milling of Ti-6Al-4V Alloy with Uncoated and cBN Coated Micro-Tools,*CIRP Annals - Manufacturing Technology*,Vol.60, pp.85-88.

Ozel, T., Llanos,I. Soriano,J. and Arrazola, P.J. (2011), 3D Finite Element Modelling of Chip Formation Process for Machining Inconel 718: Comparison of FE Software Predictions,*Machining Science and Technology*,Vol. 15, pp.21-46.

Rao, S. and Shunmugam, M.S. (2012), Analytical Modeling of Micro End-Milling Forces with Edge Radius and Material Strengthening Effects,*Machining Science and Technology*,Vol.16, pp.205-227.

Sima, M. and Ozel T. (2010), Modified Material Constitutive Models for Serrated Chip Formation Simulations and Experimental Validation in Machining of Titanium Alloy Ti-6Al-4V, *International Journal of Machine Tools and Manufacture*,Vol.50, pp.943-960.

Shen, N. and DingH. (2013), Thermo-Mechanical Coupled Analysis of Laser-Assisted Mechanical Micromilling of Difficult-to-Machine Metal Alloys Used for Bio-Implant,*International Journal of Precision Engineering and Manufacturing*,Vol.14, pp.1677-1685.

Shao, F., Liu, Z. Wan, Y. and Shi, Z. (2010), Finite Element Simulation of Machining of Ti-6Al-4V Alloy with Thermodynamical Constitutive Equation,*The International Journal of Advanced Manufacturing Technology*,Vol.49, pp.431-439.

Umbrello, D. (2008), Finite Element Simulation of Conventional and High Speed Machining of Ti6Al4V Alloy,*Journal of Materials Processing Technology*,Vol.196, pp.79-87.

Wan, Z.P., Zhu,Y.E. Liu,H.W. and Tang,Y. (2012), Microstructure Evolution of Adiabatic Shear Bands and Mechanisms of Saw-Tooth Chip Formation in Machining Ti6Al4V, *Materials Science and Engineering: A*,Vol. 531, pp.155-163.

Woon, K.S.,Rahman,M. Neo, K.S. and Liu, K. (2008), The Effect of Tool Edge Radius on the Contact Phenomenon of Tool-Based Micromachining,*International Journal of Machine Tools and Manufacture*,Vol.48, pp.1395-1407.

Yang, X. and Richard Liu,C. (1999), Machining Titanium and Its Alloys,*Machining Science and Technology*,Vol. 3, pp.107-139.

Yen, Y.C., Jain, A. Chigurupati,P. Wu,W.T.andAltan,T. (2004), Computer Simulation of Orthogonal Cutting Using a Tool with Multiple Coatings,*Machining Science and Technology*,Vol.8, pp.305-326.